Measurement of the Dissociation Rates of Hydrogen and Deuterium

Emmett A. Sutton

Citation: J. Chem. Phys. **36**, 2923 (1962); doi: 10.1063/1.1732403
View online: http://dx.doi.org/10.1063/1.1732403
View Table of Contents: http://jcp.aip.org/resource/1/JCPSA6/v36/i11
Published by the American Institute of Physics.

Measurement of the Dissociation Rates of Hydrogen and Deuterium*

EMMETT A. SUTTON†
Cornell University, Ithaca, New York
(Received April 19, 1961)

Dissociation rates for hydrogen and deuterium have been found by measuring the density profile behind an incident shock wave as a function of time in mixtures of argon and hydrogen or deuterium. The density ratio was measured using an interferometer and drum camera. Relative efficiencies of argon, the molecule, and the atom in causing dissociation have been found for each isotope by varying the relative concentrations. The dependence of the rates on temperature was measured over the range 2800°–4500°K. Association-rate constants derived from the measured dissociation-rate constants showed a $1/T$ dependence on the temperature in the case of both isotopes when the third body was the molecule or an argon atom. Derived rate constants for association when the third body is another atom were found to be much larger and to have a more involved temperature dependence.

INTRODUCTION

THE shock tube has become increasingly useful in the study of chemical reactions in the gas phase. This is because a carefully prepared sample may have its enthalpy raised a known amount very quickly compared to the time necessary for chemical reactions. As the heating is due to waves, there is no catalysis or contamination at a surface.

The kinetics of hydrogen dissociation have been studied in this experiment by measuring the density of the heated gas behind the shock wave as a function of time using a Mach–Zehnder interferometer and drum camera. Using the conservation laws of fluid mechanics and the perfect gas law, the temperature and degree of dissociation are calculated at points behind the shock wave from the density data. From this information, the rate of dissociation is found as a function of temperature and the densities of the various species present. The rate constants for the different third bodies are separated by varying the relative concentrations.

The drum-camera pictures contain information in addition to that used to determine the rate of dissociation. The initial density ratio across the shock wave is not dependent on the kinetics of dissociation for the range of temperatures and densities considered in this experiment. The measurement of this density ratio was used to verify the assumption that vibrational equilibrium is reached faster than the time difference resolved in these measurements. Subsequently, the initial density ratio was used for a check of the validity of a particular run. All runs which had a measured initial density ratio differing from the calculated values were discarded. The final-equilibrium density ratio also does not depend on the rate of the reaction. It was used to show that assuming the specific refractivity to be the same for atomic and molecular hydrogen had little effect on the analysis of these data.

The isotope effect was studied by repeating the experiment over the same temperature range using deuterium instead of hydrogen. For both isotopes the temperature range runs from approximately 2800° to 4500°K. Argon was used in various mixture ratios with the reactants to reach these temperatures.

This experiment has many similarities with earlier work done on the rate of oxygen dissociation. Byron[1] performed an oxygen experiment using the same shock tube and auxiliary equipment. Other investigators[2–5] have also studied the oxygen dissociation rate.

A different method of data reduction than had been employed previously was used. One reason was that the new method shows the scatter in the measurements in the rate constants rather than the lack of fitting the various density profiles. Another reason is that the shape of the rate constant vs temperature curve is not prejudiced by the choice of a parametric form.

DESCRIPTION OF THE EXPERIMENT

Experimental Equipment

The shock tube and its auxiliary equipment are the same as those used by Byron in a similar experiment.[1] Byron[6] and Sutton[7] have given a detailed description of the apparatus. Only enough description will be given here to make possible a discussion of the method of measurement.

Optical System and Interferometer

A Mach–Zehnder interferometer and drum camera are used to measure density variations in the test sec-

* This research was partially supported by the Mechanics Branch of the Office of Naval Research.

† Submitted in partial fulfillment of the requirements for the Ph.D. degree at Cornell University, Ithaca, New York. Present address: Hamilton College, Clinton, New York.

[1] S. R. Byron, J. Chem. Phys. **30,** 1380 (1959).
[2] J. P. Rink, H. T. Knight, and R. E. Duff, J. Chem. Phys. **34,** 1942 (1961).
[3] D. L. Matthews, Phys. Fluids **2,** 170 (1959).
[4] M. Camac and A. Vaughn, Bull. Am. Phys. Soc. **4,** 291 (1959).
[5] S. A. Losev, Doklady Akad. Nauk S.S.S.R. **120,** 1291 (1958).
[6] S. R. Byron, "Interferometric measurement of the rate of dissociation of oxygen heated by strong shock waves," thesis, Cornell University, Ithaca, New York (1958) (available from University Microfilms, Inc., Ann Arbor, Michigan).
[7] E. A. Sutton, thesis, Cornell University, Ithaca, New York, 1961 (available from University Microfilms, Inc., Ann Arbor, Michigan).

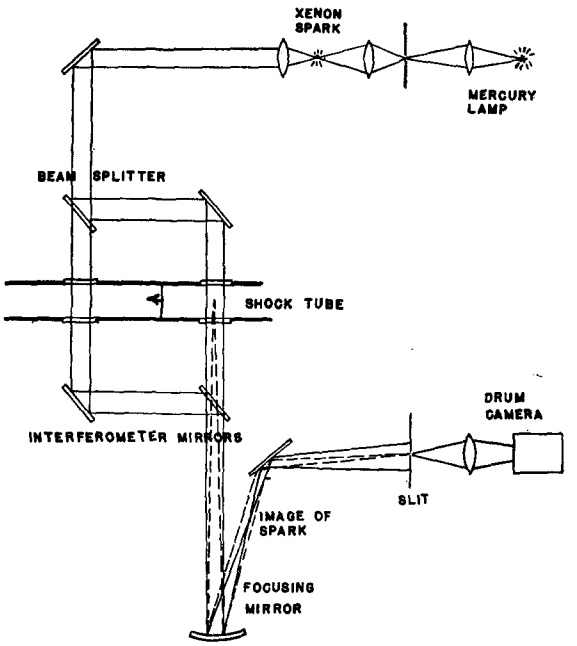

FIG. 1. The major components of the optical system.

tion of the shock tube. Using white light it is possible to identify and follow the central white light fringe. The interferometer has been placed so that each of the two beams traverses the test section of the shock tube (Fig. 1). With this arrangement, the interferometer fringe position will be a function of the density difference between the two window positions. The experiment was planned so that the reaction as viewed through the first window would be complete before the shock wave reached the second window. As the reaction zone passed the second window, the reverse of the initial fringe movement was recorded. The fringe movement due to the chemical reaction is not repeated if the shock wave has changed its strength between positions. The reproducibility of the pattern differentiates between density changes due to dissociation and density changes caused by weak waves catching up with the shock wave. In the first case, the patterns repeat; in the second, they do not.

The focusing mirror is placed so that the first test section of the shock tube forms a real image on the plane of the slit on the front of the drum camera. This means, of course, that a real image of the slit is formed in the first window of the shock tube. By choosing a long-focal-length mirror, the depth of field also allowed a reasonably sharp image of the slit to be formed at the second window. The distance between these slit images is used in measuring the speed of the shock wave.

The drum camera is run with its shutter open. The process is illuminated by a 400-μsec-duration xenon spark, initiated by the signal from a foil heat-transfer gauge mounted flush with the wall of the shock tube 6 in. upstream from the first test section.

The data for each run of the experiment consist of the following measurements. First, the pressure and species concentration of the gas used in the test section of the tube is determined. Second, an interferogram is taken using the drum camera. From this photograph the rest of the measurements are made. These measurements will be discussed below.

The hydrogen and argon were mixed in a mixing chamber while the partial pressures of each gas were measured on a mercury manometer. These pressures were measured with an accuracy of $\frac{1}{4}$ mm Hg. The smallest pressure measured during the mixing process or in the shock tube was about 25 mm Hg. Therefore the maximum relative errors in the pressure measurement due to measurements while mixing, and in the measurement of the sample pressure in the shock tube, are together of the order of 2%. Since the density after the shock wave is a multiple of the initial density, this same relative error will hold for all the measured densities in the experiment.

The source of impurities in the gas sample was different for the two isotopes. In the case of the hydrogen and argon used in this experiment, total impurities of the bottled gas were less than 58 ppm. Most of the impurities were due to the residual gas in the system and the gas which leaked into the system during mixing and before the experiment was completed. An experimental run was made only if, after the leak rate was measured, it was seen that the residual gas plus that which would leak in after the pumping had been stopped would result in a maximum partial pressure of impurities less than 5×10^{-3} mm Hg. Since the runs were made with initial pressures from 2 to 10 cm Hg, all impurities from leaks and internal sources in the tube were less than 0.03%.

The bottled deuterium was not as pure as the hydrogen or argon. A mass-spectrometric analysis on the bottle gave 99% deuterium with most of the remaining impurity being H_2 and HD. The impurity level due to leaks was the same as for hydrogen.

The test sample was allowed to stand in the mixing vessel for about 20 min before being introduced into the shock tube. The sample was then introduced into the shock tube and allowed to stand for another 10 min before the run to allow it to reach a uniform temperature in equilibrium with the walls of the shock tube.

Drum-Camera Speed

A capacitative pickup on the drum camera has its signal superimposed on a circular Lissajou figure, formed by putting a 60-cycle line frequency signal on both the vertical and horizontal deflections. If this figure seems to rotate so that one pip moves to the position where another has been in 1 sec, the difference in the drum camera speed is 1 rps. This allows the drum camera to be set accurately relative to the line frequency used as the standard. The instantaneous varia-

tion of the line frequency was no more than 0.1 cps. For these experiments, therefore, the drum-speed error was less than $\frac{1}{2}$ rps when the camera was being run at 300 rps. Therefore, the error in the time on the film was less than $\frac{1}{4}\%$.

Measurements from the Drum-Camera Photograph

Introduction

A sample drum-camera interferogram is given in Fig. 2. A labeled drawing showing the various features of this picture follows it in Fig. 3. In analyzing the data the resolution of the center of the fringe limited measurement of the fringe position. It was found that the resolution of the fringe position was no better than about $\frac{1}{40}$ of the fringe spacing. As the fringes usually moved about three times their spacing, the density ratio could be determined with an error less than 1%.

In those runs in which things happen quickly, the time resolution of the center of the fringe is better than the time which the film takes to cross the image of the slit. For most of the runs, the exposure time of a point on the film is about one microsecond. For the fast runs, time resolution is better than $\frac{1}{10}$ μsec. This is true in those portions of the pictures where the gradient is steep while the curvature is small. The fringe patterns seen in the faster runs of this experiment fit these conditions well. In the slower runs where the gradients are smaller the time resolution falls off to the 1-μsec level.

Part of the error in the measurement of the shock-wave speed depends on the time resolution. The errors in the measurement of the spacing of the slit images in the shock tube, in the measurement of horizontal distances on the film, and time resolution are together less than $\frac{1}{4}\%$. Coupled with a possible error of $\frac{1}{4}\%$ in the measurement of the drum-camera speed, the shock-wave-velocity measurement has an error less than $\frac{1}{2}\%$.

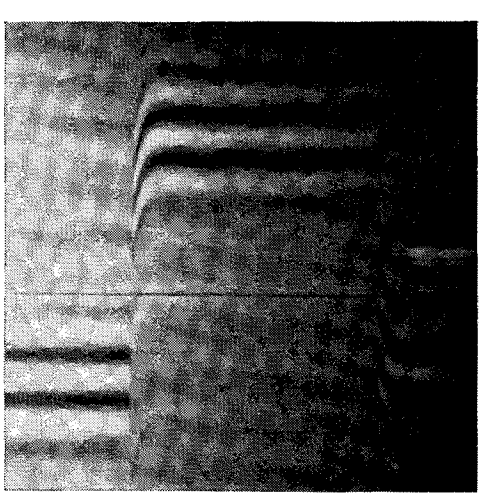

FIG. 2. The drum-camera photograph. The same run was used for the sample of Fig. 4.

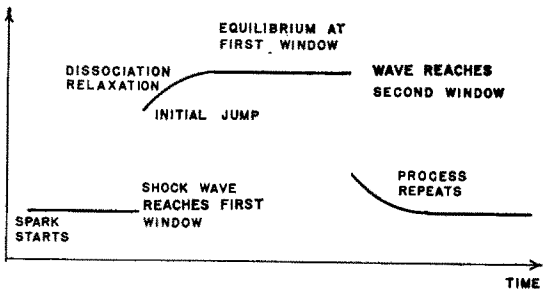

FIG. 3. Details of the drum-camera picture.

The fringe spacing for each run was found by measuring the distance between monochromatic-light fringes which were included on each drum-camera picture for calibration. By measuring the distance of 10 fringes, the error in this measurement is held to less than 1%. The fringe spacing and the measurement of the fringe position is then used to calculate the number of fringe shifts as a function of time behind the shock wave.

The number of fringe shifts is related to the density by

$$\Delta N = (\mathrm{GD})\,(d\rho_1/\lambda\rho_0)\left[(\rho/\rho_1)-1\right],$$

where (GD) is the Gladstone–Dale constant for the gas mixture and λ is the wavelength of the monochromatic light used for calibration. For this experiment λ was 5461 A. The width of the test section is given by d, while ρ_0 is standard density and ρ_1 is the initial density in the shock tube. The same value for the Gladstone–Dale constant was used for both hydrogen and deuterium. It was assumed that dissociation into hydrogen atoms did not affect the specific refractivity of the gas. Although there may be an effect due to a different specific refractivity for hydrogen atoms, it was not noticeable from a comparison of the equilibrium densities reached with those calculated (Fig. 5). Using this equation and the interferogram giving the number of fringe shifts as a function of time results in a profile of the density ratio measured at the first window as a function of time. A sample profile for one run is shown in Fig. 4.

The measured density ratio immediately behind the shock wave and after the dissociation has reached equilibrium were then plotted on the equilibrium curves (a sample curve is given in Fig. 5). These data were used to test two assumptions. The initial density ratio is used to find whether the vibration has come to equilibrium immediately behind the shock wave. The measured initial density ratios scattered about the curve calculated using a value for the internal energy of hydrogen molecules for which vibration was at its equilibrium value. Therefore, it was assumed that vibrational equilibration was faster than any time difference which could be resolved in these measurements. The final density ratio was used, as previously mentioned, to check whether the value of the Gladstone–Dale constant changed significantly as a result

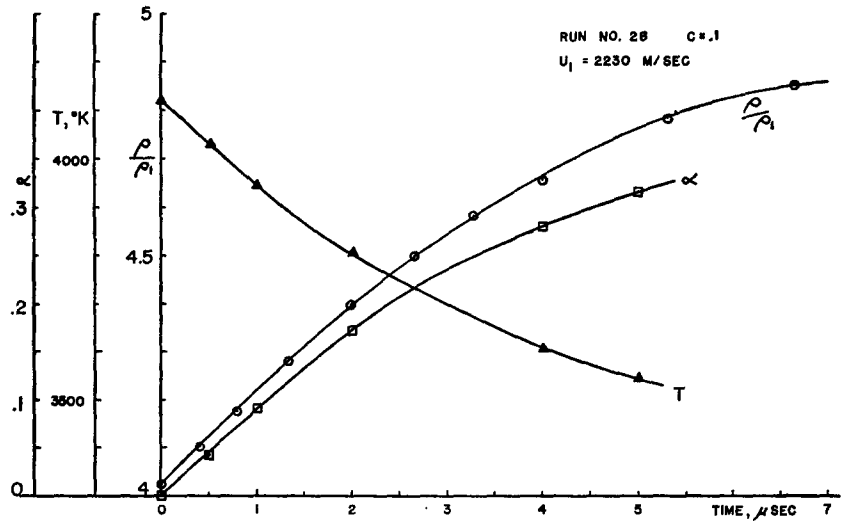

FIG. 4. Conditions behind the shock wave.

of hydrogen dissociation. It did not. Alpher and White[8] used this same method to measure the specific refractivity of atomic oxygen.

As the measured values of the initial density ratios fit the calculated curves quite well, their scatter was used as a further check of the data. Any run whose initial density ratio differed by more than 2% from the calculated densities was not analyzed further. Furthermore, if the measured value of the initial density ratio was greater than the calculated value the final density ratio was also required to be greater than its calculated value. This last condition has been imposed to be consistent with the previous discussion of possible errors in the measurement of the density. The errors due to faulty measurement of the initial pressure, the fringe spacing, and the measurement of the fringe position before the shock wave give a shift in the same direction at each check point.

After the two tests a correction was made to those runs which were found acceptable. The error in the measurement of the shock-wave speed is less than the error in the measurement of the density ratios. Since the equilibrium curves were calculated using the exact equations and what is believed to be the best values of the thermodynamic properties of hydrogen available, these equilibrium values were then used to get a factor by which the measured values of the density ratio were multiplied. The correction factor was the ratio of the calculated density ratio immediately behind the shock wave to the observed initial density ratio. This correction makes the less exact measurement of the density ratios consistent with the measurement of the shock-wave speed. It should be emphasized, however, that this correction was only made for those runs which were already within the allowable range of error.

In all, 130 runs were made. After applying these tests,

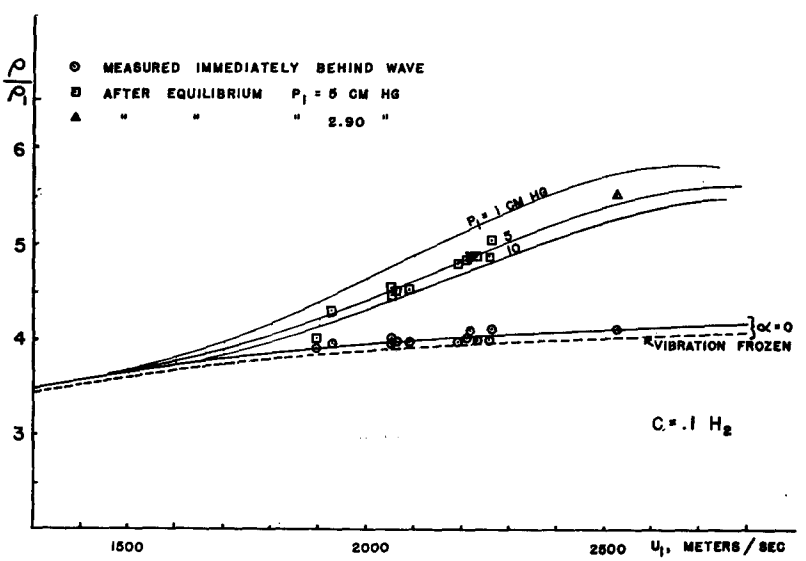

FIG. 5. The equilibrium density ratios across a shock wave.

[8] R. A. Alpher and D. R. White, Phys. Fluids **2**, 153, (1959).

20 runs for hydrogen and 15 runs for deuterium were found acceptable.

ANALYSIS OF THE EXPERIMENT

The analysis of the experiment is separated into two parts. The first is the calculation of the properties behind the shock wave for several states of equilibrium and quasi-equilibrium. The states of quasi-equilibrium are those for which certain modes, such as the translational and rotational have reached equilibrium, while other modes such as dissociation are still essentially frozen. These computations are not used directly in the evaluation of the rates. They are used in evaluating the validity of the various experimental runs, checking the validity of assumptions, and making small corrections to the measurements as stated in the section on measurements. The second part of the analysis is the computation of the various rate constants from the experimental data.

Calculation of the Various Equilibrium Properties behind the Shock Wave

In a coordinate system whose origin is fixed in the shock wave, the equations for the conservation of mass, momentum, and energy are

$$\rho_1 u_1 = \rho u, \tag{1}$$

$$p_1 + \rho_1 u_1^2 = p + \rho u^2, \tag{2}$$

$$h_1 + \tfrac{1}{2}u_1^2 = h + \tfrac{1}{2}u^2, \tag{3}$$

where p, ρ, and u are, respectively, the pressure, density, and velocity, and h is the specific enthalpy. The subscript 1 will always denote conditions before the shock wave. The specific enthalpy is given by

$$h = \Re T\{\tfrac{5}{2} + c[\tfrac{5}{2}\alpha + \eta(1-\alpha)]\} + \Re c\alpha T_{\text{dis}}, \tag{4}$$

where c measures the initial ratio of hydrogen molecules to the total number of molecules. T_{dis} is the equivalent temperature derived from the dissociation energy; η is a function of the temperature which measures the contribution to the enthalpy of the internal energy states of the hydrogen molecule. α measures the relative amount of dissociation, and is defined by

$$\alpha = n_{\text{H}}/(2n_{\text{H}_2} + n_{\text{H}}),$$

where n is the molar density, the species being given by the subscript. $\Re$ is the specific gas constant, related to the universal gas constant R by

$$\Re = R/M,$$

where M is the molecular weight of the undissociated gas mixture. The equation of state for a dissociating gas is

$$p = \rho \Re T(1 + c\alpha). \tag{5}$$

Finally, the equilibrium dissociation is given by the mass action law

$$p_{\text{H}}^2/p_{\text{H}_2} = K_p.$$

In terms of the variables used in this analysis, this becomes

$$\alpha^2/(1-\alpha) = K_p \rho_1 T_1/\rho T 4 c p_1. \tag{6}$$

The evaluation of T_{dis}, η, and K_p was done using the thermodynamic properties of Hydrogen as calculated by Woolley, Scott, and Brickwedde.[9] The dissociation temperatures for both hydrogen and deuterium were calculated from the data in the Woolley, Scott, and Brickwedde article. The thermodynamic properties of deuterium are those tabulated in Haar, Friedman, and Beckett.[10]

A solution of these equations was obtained for several initial values of c and p_1. From these values, ρ/ρ_1 was plotted as a function of shock-wave velocity u_1 for several values of c and p_1. These are the curves for the equilibrium-dissociation-density ratio behind a normal shock wave. The curves for the 10% hydrogen case are given in Fig. 5.

There are also states of quasi-equilibrium whose computation proves very useful. Immediately behind the shock wave, if the time is too short for any appreciable dissociation, there will be an appropriate density ratio and temperature which can be computed as a function of u_1. The same equations are solved setting $\alpha = 0$. When found, these values are also plotted.

Finally, this same calculation has been made for not only the dissociation frozen, but also the vibrational excitation frozen. This is done by setting $\eta = 1$ for all T except T_1 and again solving the equations and plotting the results. The results of this calculation were used in evaluating the assumption that the vibrational degrees of freedom do not lag.

These three curves for ρ/ρ_1 vs u_1 give the density ratios immediately behind the shock wave, after vibration has come to equilibrium, and after dissociation has come to equilibrium. Their use is discussed in the section on measurement and data collection.

CALCULATION OF THE RATE CONSTANTS

For dissociation to occur, the hydrogen molecule must have a collision with another body or group of bodies. If this collision is with one other body, the collision is called bimolecular, and if the collision is with two other bodies simultaneously, it is called termolecular. The frequency of these different collisions depends on a power of the density; bimolecular collisions have their frequency proportional to the square of the density, while that of termolecular collisions is proportional to the cube of the density, and so on. In order to conserve both energy and momentum in a collision if no photons are emitted or absorbed, it can be shown that a bimolecular reaction is the lowest-order dissociation reaction and a termolecular reaction the lowest-

[9] H. W. Woolley, R. B. Scott, and F. G. Brickwedde, J. Research Natl. Bur. Standards **41**, 379 (1948). This is the description. The tabulation is in NBS Circ. 564.

[10] L. Haar, A. S. Friedman, and C. W. Beckett, NBS monograph #20.

order association reaction that is allowed. An assumption here made and later shown to be valid, is that at the densities of this experiment, only the lowest-order reactions need be considered. If this is the case, γ_{H_2}, the net molar rate of production of hydrogen molecules by chemical means, can be written as

$$\gamma_{H_2}=k_1 n_H{}^3+k_2 n_H{}^2 n_{H_2}+k_3 n_H{}^2 n_{Ar}-k_4 n_{H_2} n_H - k_5 n_{H_2}{}^2-k_6 n_{H_2} n_{Ar}, \quad (7)$$

where, as usual, the n's are the molar densities of the various species. This equation will be taken as defining the rate constants k_i. When referring to these rate constants, k_4, for instance, will be called the dissociation rate constant for hydrogen with hydrogen atoms the third body. If the assumption about the molecularity and hence the density dependence of the reaction is right, the k's will be functions of the temperature only.

In Penner,[11] the relation for γ_{H_2} in terms of flow variables is given:

$$(Dn_{H_2}/Dt)+[\partial(n_{H_2}V_{H_2})/\partial x]-(n_{H_2}/\rho)(D\rho/Dt)=\gamma_{H_2}. \quad (8)$$

V_{H_2} is the diffusion velocity of hydrogen molecules. It is very small compared to the other velocities in this experiment and will be shown to be negligible in the dissociation region behind the shock wave, where the measurements of γ_{H_2} have been made. From Penner,[11] the relation giving the diffusion velocity is

$$V_{H_2}=-D_{H_2-Ar}\left[\frac{\partial}{\partial x}\left(\ln\frac{\rho_{H_2}}{\rho}\right)+\left(\frac{\rho_{H_2}}{\rho M_{H_2}}+\frac{\rho_{Ar}}{\rho M_{Ar}}\right)\times(M_{Ar}-M_{H_2})\frac{\rho_{Ar}}{\rho}(\partial/\partial x)(\ln\rho)+\frac{(M_{Ar}\rho_{H_2}/\rho+M_{H_2}\rho_{Ar}/\rho)^2}{M_{Ar}M_{H_2}}\times\mathcal{K}_T\left(\frac{\rho}{\rho_{H_2}}\right)\frac{\partial}{\partial x}(\ln T)\right], \quad (9)$$

where D_{H_2-Ar} for hydrogen–argon mixtures is 0.77 and $\mathcal{K}_T$, the thermal-diffusion coefficient, is approximately 0.1 in these cases. The reaction zone is approximately 10 cm and the fastest changing quantity is the density ratio ρ_{H_2}/ρ. The first term in the brackets can be estimated with the approximation that half the hydrogen is dissociated in that distance.

$$\frac{\partial}{\partial x}\left(\ln\frac{\rho_{H_2}}{\rho}\right)\sim\frac{\Delta\ln\rho_{H_2}/\rho}{\Delta x}=\frac{0.69}{10}.$$

This will make the diffusion velocity less than 1 cm/sec even when the rest of the terms are included. As the other velocities in the experiment are on the order of 10^5 cm/sec, the diffusion velocity is seen to be negligible.

[11] S. S. Penner, *Chemistry Problems in Jet Propulsion* (Pergamon Press, New York, 1957).

In terms of the flow variables used in this discussion, where the molar density is given by

$$n_{H_2}=c(1-\alpha)\rho/M, \quad (10)$$

Eq. (8) becomes, after performing the algebraic cancellations,

$$\gamma_{H_2}=-(c\rho/M)(D\alpha/Dt). \quad (11)$$

In the shock-wave fixed-coordinate system, where conditions are steady for a nondecaying shock wave,

$$\gamma_{H_2}=-(c\rho/M)u(\partial\alpha/\partial x).$$

Using the mass-continuity equation [Eq. (1)] this becomes

$$\gamma_{H_2}=-(c\rho_1/M)u_1(\partial\alpha/\partial x). \quad (12)$$

In the shock–fixed-coordinate system, the gas ahead of the shock wave is moving into it with speed u_1. In the laboratory coordinates, the gas ahead of the shock wave is at rest and the shock wave moves into it with speed u_1. The change of coordinates is made using the following relationships:

$$x'=x-u_1 t, \qquad t'=t, \quad (13)$$

where the primed quantities refer to the laboratory coordinates and the unprimed quantities refer to the shock-wave fixed coordinates. The derivatives in the different coordinates are related by

$$(\partial/\partial t)=(\partial/\partial t')+(-u_1)(\partial/\partial x')=0, \quad (14)$$

$$\partial/\partial x=\partial/\partial x'. \quad (15)$$

Using Eq. (14) to find $\partial/\partial x'$ in terms of $\partial/\partial t'$, and substituting in Eq. (15), the relation between the spatial derivative in the shock-fixed coordinates and the time derivative at a point in the laboratory is found

$$\partial/\partial x=(1/u_1)(\partial/\partial t'). \quad (16)$$

Therefore, Eq. (12) becomes

$$\gamma_{H_2}=-(c\rho_1/M)(\partial\alpha/\partial t') \quad (17)$$

in laboratory coordinates.

However, it was not α but ρ/ρ_1 which is measured by the interferometer. Therefore, the conservation equations must be used to calculate α and the temperature as a function of time. Equations (1–5) still hold for the nonequilibrium case. These equations coupled with the measurement of the density will allow α and T to be found. They were first reduced to two simultaneous equations for convenience:

$$\alpha=\frac{h_1/\mathfrak{R}+\frac{1}{2}(u_1{}^2/\mathfrak{R})[1-(\rho_1/\rho)^2]-T(\frac{5}{2}+c\eta)}{cT(\frac{5}{2}-\eta)+cT_{dis}}, \quad (18)$$

$$T=\frac{\rho_1}{\rho}\left[\frac{T_1+(u_1{}^2/\mathfrak{R})(1-\rho_1/\rho)}{1+c\alpha}\right]. \quad (19)$$

This calculation is made at enough points along the

curve for a given run to allow one to plot α and T versus time. A sample run has been plotted in Fig. 4.

Having found these properties as a function of time, γ_{H_2} may be evaluated at any point along the curve. Immediately after the shock wave, as α will be zero, only dissociation caused by hydrogen molecules and argon atoms will be taking place. At this point, the rate constants k_5 and k_6 may be evaluated. By performing the experiments at different mixture ratios, it is possible to resolve these two rate constants.

A digression is necessary at this point. It has become a common practice in the reporting of measured rate constants, not to report the measured dissociation-rate constants, but to report the association-rate constants which are derived from them using the equilibrium constant. Each dissociation-rate constant is related to the association-rate constant for the inverse reaction.

$$k_4/k_1=k_5/k_2=k_6/k_3=K_c, \tag{20}$$

where K_c is the molar equilibrium constant related to K_p by

$$K_c=K_p/RT. \tag{21}$$

In using this relation, there are some assumptions made which will be discussed later.

In Figs. 6 and 7, the joint rate constants for hydrogen and deuterium mixtures have been plotted using the experimental data. These rate constants as measured are just the molar density weighted averages of the molecular rate constants k_2 and k_3.

$$k_c=ck_2+(1-c)k_3. \tag{22}$$

The experiments performed with 10% and 30% mixture ratios were used to find the values of k_2 and k_3. The data collected in 3% mixtures in the case of hydrogen were not used in evaluating k_2 and k_3 as there was not enough of it. If $k_{0.03}$ is calculated from the already determined values of k_2 and k_3, it will be seen that the few points available for this mixture ratio agree with the other data within the range of their scatter.

CALCULATION OF THE ATOM RATE CONSTANT

Assuming that the dissociation-rate constants k_5 and k_6 and their respective inverse-reaction-rate constants, k_2 and k_3 are known, it is then possible to give a formula relating γ_{H_2} and the rate constants in which the atoms are the third body. From Eqs. (7) and (17):

$$-(c\rho_1/M)(\partial\alpha/\partial t)=k_1n_H{}^3+k_2n_H{}^2n_{H_2}+k_3n_H{}^2n_{Ar}-k_4n_{H_2}n_H-k_5n_{H_2}{}^2-k_6n_{H_2}n_{Ar}. \tag{23}$$

The dissociation-rate constants are eliminated from this equation using Eq. (20). The molar densities are given by

$$n_{Ar}=(1-c)(\rho/\rho_1)(\rho_1/M),$$
$$n_{H_2}=c(1-\alpha)(\rho/\rho_1)(\rho_1/M),$$
$$n_H=2c\alpha(\rho/\rho_1)(\rho_1/M).$$

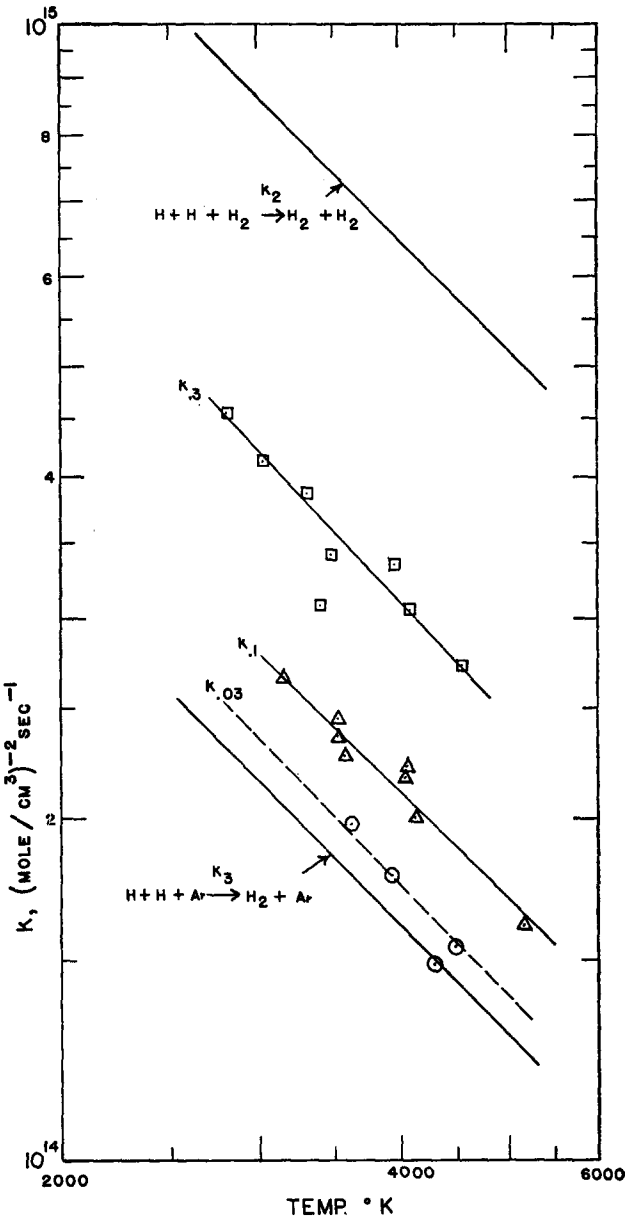

FIG. 6. Association-rate constants of hydrogen for the third bodies H_2 and Ar.

Making these substitutions, it is then possible to solve for k_1.

$$k_1=[2K_cc^2\alpha(1-\alpha)-(\rho/\rho_1)(\rho_1/M)(2c\alpha)^3]^{-1}\times\{c(\partial\alpha/\partial t)/(\rho/\rho_1)^2(\rho_1/M)-k_2[K_cc^2(1-\alpha)^2-(\rho/\rho_1)(\rho_1/M)(2c\alpha)^2c(1-\alpha)]-k_3[K_c(1-c)c(1-\alpha)-(\rho/\rho_1)(\rho_1/M)(2c\alpha)^2(1-c)]\}. \tag{24}$$

This equation was used to calculate this rate constant at one or more points along the α curve in a given experiment. The results are shown in Fig. 8.

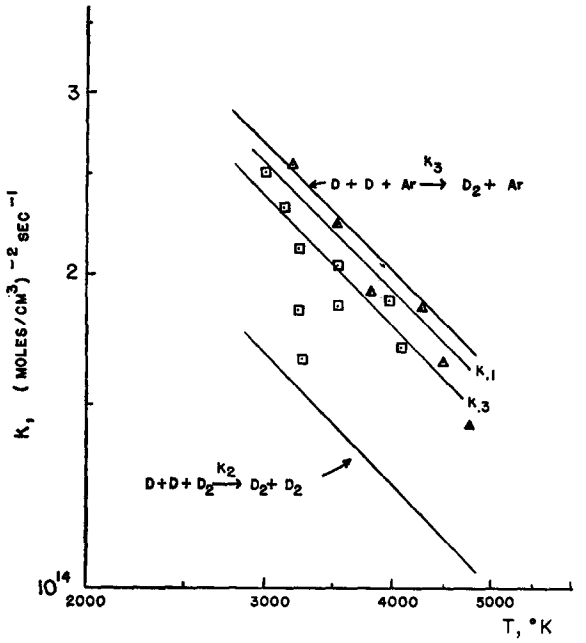

FIG. 7. Association-rate constants of deuterium for the third bodies D_2 and Ar.

DISCUSSION

Validity of the Various Approximations

Several simplifying assumptions have been made in the analysis of this experiment. Major assumptions were that the dissociation reactions were bimolecular, that the association-rate constants could be derived from the dissociation-rate constants using the equilibrium constant, and that, in the calculation of the temperature, vibration is fully excited to its equilibrium value.

If the vibrational degrees of freedom were to lag, it would not only make the calculation of the temperature wrong, but the use of the equilibrium constant to compute the association rate would not be justified. The equilibrium curves (Fig. 5) were used to show that any lag in the vibrational equilibration cannot be noticed in this experiment. The density ratio immediately behind the shock wave was calculated in all cases for the vibrational degrees of freedom both fully equilibrated and frozen at their room-temperature value. It was apparent from the data that all the initial density increases across the shock wave are those which would be expected if the vibration were fully equilibrated. This was most evident for the 30% mixture ratios. Since the biggest temperature gradient anywhere in the flow is that across the shock wave, there will be no measurable effect of a lagging vibrational degree of freedom anywhere in the experiment.

The use of the equilibrium constant to relate the dissociation-rate constant to the association-rate constant is justified only if the microstates of both products and reactants have an equilibrium distribution for eth given temperature. This situation could only be verified if one were to know the entire population of states or to measure both the dissociation and association rate constants. However, departure from an equilibrium distribution among the vibrational levels is one of the more likely cases. Therefore, showing that there was no measurable vibrational lag was important for the use of the equilibrium constant.

In assuming that a reaction has a certain molecularity, the density dependence of the reaction is assumed. The assumption is checked by showing that the rate constants calculated on the basis of the assumed molecularity do not depend on the density. This was done by varying the initial densities of several runs. Within the scatter of the rate constants, varying the density of the experiments by a factor of four had no apparent effect on their values. Initial pressures in these experiments ranged from 2.5 to 10 cm Hg. If the scatter in the data is taken to be on the order of 10%, the effects of reactions of other molecularities must be less than 2.5% if all the scatter in the data were due to this cause.

The error expected in the data should be about 10% if caused by the various sources mentioned earlier. The average scatter in the case of hydrogen from the curves drawn through the data points is seen to be less than 10%. For deuterium the scatter in the data is seen to be greater than for the lighter isotope. The experimenter finds this relative increase in the error for the deuterium hard to explain as the conditions were the same, except for the larger impurities level in the deuterium, for both isotopes.

SUMMARY AND REMARKS

The results of the experiment have been presented in Figs. 6–8. The association-rate constants for the molecules and argon atoms as the third bodies showed

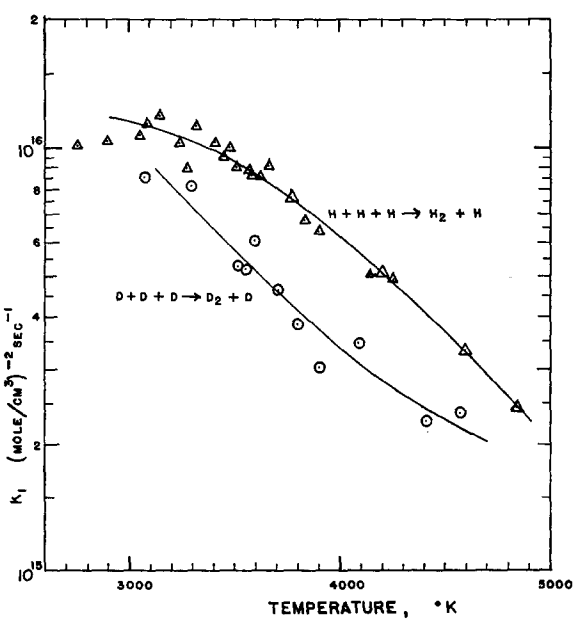

FIG. 8. The association-rate constants for hydrogen and deuterium with the atoms as third bodies.

a simple temperature dependence. These rate constants could be well represented by $k_i = A_i/T$ throughout the entire temperature range over which they were measured. For the ordinary isotope of hydrogen, the efficiency of the hydrogen molecule was seen to be greater than that of the argon atom as a third body in the reaction. For deuterium, however, these roles were reversed; the rate constant for the argon atom was greater than that for the deuterium molecule. The rate constant for association with argon the third body was found to be greater in the case of deuterium than for the lighter isotope.

The association-rate constants for the reaction where the hydrogen and deuterium atoms were the third bodies showed several differences from the rate constants where the molecules and argon were the third bodies. For both isotopes, these rate constants were at least an order of magnitude larger than the rate constants for the molecules and argon as third bodies. They were not simple functions of the temperature. Both of these atom rate constants showed a much steeper decrease with increasing temperature than the rate constant for the molecules. For hydrogen, this atom rate constant below about 3400°K decreases as $1/T^{\frac{3}{2}}$. Above this temperature, this rate constant decreases much more quickly, approximately as $1/T^4$. Deuterium also showed this sharp decrease, but its slower rate of decrease came at the high-temperature limit of its range. The steepest part of the curves in both cases comes at temperatures where the vibrational heat capacity is halfway between its quantum restricted and classical values.

ACKNOWLEDGMENTS

The completion of this work would not have been possible without the help of many people. Chief among them are Dr. Stanley Byron who had improved the shock tube used in this study and gave a great deal of help to the author in the beginning phases of this work. The laborious calculations were handled by Mrs. Ann Pugh and Miss V. Ann Walbran. The author would especially like to thank Professor Edwin L. Resler for the many helpful discussions while this work was being done.

THE JOURNAL OF CHEMICAL PHYSICS VOLUME 36, NUMBER 11 JUNE 1, 1962

Microwave Spectrum of Bromocyclobutane*

W. G. ROTHSCHILD† AND B. P. DAILEY
Department of Chemistry, Columbia University, New York 27, New York

(Received January 11, 1962)

Rotational transitions of four isotopic species of bromocyclobutane have been observed. For $C_4H_7Br^{79}$,

$$\alpha\text{-}C(BrH)\text{—}\beta\text{-}C(H_2)\text{—}\gamma\text{-}C(H_2)\text{—}\beta\text{-}CH_2$$

or

$$C_\alpha BrH - C_\beta H_2 - C_\gamma H_2 - C_\beta H_2,$$

the rotational constants are $A = 10\,003.4 \pm 13$ Mc, $B = 1629.41 \pm 0.03$ Mc, $C = 1488.48 \pm 0.03$ Mc; for $C_4H_7Br^{81}$, $A = 10\,002.6 \pm 13$ Mc, $B = 1615.14 \pm 0.03$ Mc, and $C = 1476.50 \pm 0.03$ Mc. The values for the α-deuterated compound are, for $C_3H_6CDBr^{79}$, $A = 9534.7 \pm 13$ Mc, $B = 1613.67 \pm 0.03$ Mc, and $C = 1486.24 \pm 0.03$ Mc; for $C_3H_6CDBr^{81}$, $A = 9533.4 \pm 13$ Mc, $B = 1599.55 \pm 0.03$ Mc, and $C = 1474.24 \pm 0.03$ Mc. A set of structural parameters which reproduce these constants within 1.8 Mc were obtained with an electronic computer: bond distances C_α—$C_\beta = 1.540 \pm 0.003$ Å, C_β—$C_\gamma = 1.548 \pm 0.003$ Å, C—Br = 1.939 Å, C—H = 1.096 Å, and C—D = 1.087 Å; bond angles $C_\beta C_\gamma C_\beta = 88°\ 06' \pm 08'$, $C_\beta C_\alpha C_\beta = 88°41' \pm 08'$, $HC_\gamma H = 110°44'$, $HC_\beta H = 108°44'$, $HC_\alpha Br = 111°$, angle of $C_\beta C_\alpha C_\beta$ plane with C—Br = $131°00' \pm 08'$, and dihedral angle = $29°22' \pm 08'$ (the dihedral angle is the angle made by the normals of the $C_\beta C_\alpha C_\beta$ and $C_\beta C_\gamma C_\beta$ planes). The quadrupole-coupling constant of $C_4H_7Br^{79}$ along the C—Br bond direction is 512.2 ± 5.0 Mc and the asymmetry parameter η_{bond} is -0.002 ± 0.014; these figures yield an upper limit of about 1% double-bond character due to conjugation of the Br atom with the C ring and an ionicity of the halogen bonding orbital of 25% assuming 8.6% s character. From frequency and intensity measurements of rotational satellites a low-lying vibrational mode was identified. Its effect is a displacement of all atoms in the molecule (out-of-plane bending). Its first and second excited states are 120 ± 25 and 251 ± 56 cm^{-1}, respectively, above ground level. The three lowest levels of the vibrational mode were shown to be large-amplitude vibrations of the molecule about a dynamical equilibrium dihedral angle of 25° to 29°. Highly excited vibrational states, which cause increasing planarity of the carbon ring, are expected to lead to tunneling through the potential barrier to the less stable "axial" isomer of bromocyclobutane. The existence of the axial isomer by direct observation could not be established due to instrumental difficulties.

INTRODUCTION

THE structure of cyclobutane has been a subject of much recent research. The cyclobutane ring is said to be strained since the C—C—C bond angle is markedly different from the tetrahedral value. The maximum possible value of this angle would be 90° for a planar ring. However, the mutual repulsion of the hydrogen atoms would be less in a "puckered," nonplanar ring, having C—C—C bond angles less than 90°.

From infrared data, Wilson[1] has reported a planar

* This research was supported in part by the U. S. Air Force through the Office of Scientific Research and by the National Science Foundation.

† Present address: Scientific Laboratory, Ford Motor Company, Dearborn, Michigan.

[1] T. P. Wilson, J. Chem. Phys. **11**, 369 (1943).